PHYSICAL REVIEW A VOLUME 24, NUMBER 3 SEPTEMBER 1981

Angular distribution of photoelectrons of Xe 5p spin-orbit components between 20 and 105 eV

Manfred O. Krause and Thomas A. Carlson
Oak Ridge National Laboratory, Oak Ridge, Tennessee 37830

Pamela R. Woodruff
Synchrotron Radiation Center, University of Wisconsin, Stoughton, Wisconsin 53589

(Received 8 May 1981)

With the use of synchrotron radiation, the β parameters of the Xe 5p components have been measured between 20 and 105 eV in a regime in which both relativistic and many-body effects are important. The experimental β values of $^2P_{3/2}$ and $^2P_{1/2}$ are found to be in good accord with the relativistic random-phase-approximation (RRPA) theory, but only in fair agreement with the Dirac-Fock prediction. Similarly, the branching ratio $\sigma(^2P_{3/2})/\sigma(^2P_{1/2})$ agrees well with the RRPA. However, the Dirac-Fock model accounts satisfactorily for the difference in the β values of the components indicating similar many-body effects acting on both components. A brief description is given of the new gas-phase angle-resolved electron-spectrometry system used in this work.

INTRODUCTION

The photoeffect in the outer regions of xenon serves well as a probe of both the many-body and relativistic aspects of atomic structure and dynamics. This holds true especially if, in the measurement of partial cross sections and asymmetry parameters, the spin-orbit components are resolved and regions of Cooper minima and resonances are covered. In this work, we measured, with the aid of synchrotron radiation, the angular distributions of the Xe 5p photoelectrons in the energy range from 20 to 105 eV. Because the measurement resolved the $^2P_{3/2}$ and $^2P_{1/2}$ components and covered the regions of the Cooper minimum of the 5p cross section and the maximum of the 4d cross section, this study represents one of the more sensitive tests of the theoretical models and allows an assessment of the relative importance of the many-body and the relativistic effects.

Previous work on the photoionization of xenon and other noble gases has been summarized by Johnson and Cheng[1] and by Krause.[2] The experimental studies most closely related to this work are those by Dehmer *et al.*,[3] who reported the asymmetry parameter β for both 5p components at the photon energies available from He and Ne discharge lamps, by Torop *et al.*,[4] who measured the average β value for the 5p doublet between 60 and 130 eV, and by Wuilleumier *et al.*,[5] who determined the $^2P_{3/2}/^2P_{1/2}$ branching ratio from 18 to 105 eV. The theoretical predictions of the various properties of photoeffect in xenon were made in the single-particle Dirac-Fock (DF) model[6] and in the many-body models of the nonrelativistic random-phase approximation (RPA)[7] and the relativistic random-phase approximation (RRPA).[8] Furthermore, the many-body calculations consider the effects of different interchannel interactions, such as the interactions between the 5p and 5s photoionization channels and those between the 5p, 5s, and 4d channels.

EXPERIMENTAL APPARATUS AND PROCEDURE

The electron-spectrometry system used in conjunction with synchrotron radiation (ESSR) and a toroidal grating monochromator (TGM) is shown in Fig. 1. This is a new ESSR system designed specifically for the windowless measurement in the gas phase of angular distributions of electrons emitted from atoms and molecules. Two 51-mm-radius, 164-degree spherical sector electrostatic analyzers are used as the dispersive elements, each with an adjustable resolution, $\Delta E/E$, from 0.3 to 2%. The analyzers, which are mounted at right angles to each other on a rotatable platform supported by a sapphire ball bearing, can be rotated in tandem, manually at present, through an angle of 270° about the photon beam. The angular resolution is 4°, as determined by a set of Mo apertures mounted in the source cell. The source cell which can be biased accepts both permanent gases, used for study or calibration, and atomic vapors produced in an oven. Three nested 1-mm magnetic shields, one rotating with the analyzers and two fixed, ensure a virtually field-free path for the electrons. All materials, except some electrical components, are suitable for ultrahigh-vacuum operation.

Particular attention was given to the pumping system to protect the photon source, especially the monochromator, from deleterious gas loads and deposits and, at the same time, allow the electron source to be maintained at a pressure of 10^{-2} to 10^{-1} Pa. Because the vacuum in the monochromator, about 2×10^{-8} Pa, should not be compromised, a pressure differential of better than

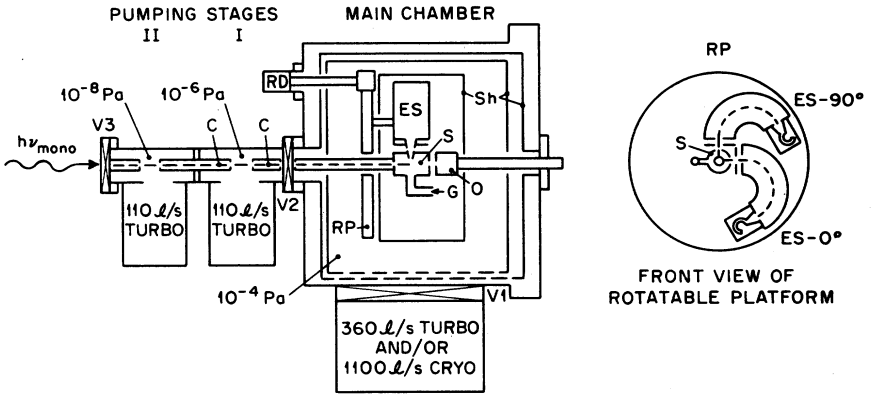

FIG. 1. Sketch of ESSR system, showing two analyzers (ES) mounted on a rotatable platform (RP) with drive (RD) around the electron source (S), which allows the use of a gas (G) or an atomic beam from an oven (O); three magnetic shields (Sh) are used and three valves ($V1$ to $V3$) separate components; typical pressures are indicated at an estimated pressure of 10^{-2} Pa in source (S) and the high impedances provided by the capillaries (C).

10^7 is needed. We achieved this by using two differential pumping stages, each pumped by a 110-l/s turbomolecular pump, and interposing a 30-cm-long 2-mm capillary between the cell and the first stage, a 14-cm-long 4-mm capillary between the first and second stages, and a 5-cm-long masked (3×6 mm^2) 10-mm tube between the second stage and the monochromator. A slot cut in the first capillary provided additional pumping through the main chamber, which can be evacuated with either a 360-l/s turbomolecular pump or a 1100-l/s cryopump or both. Using only the turbopumps, the following pressures were recorded with ionization gauges for an estimated pressure of $(2-6)\times 10^{-2}$ Pa of He or Xe in the source cell (base pressures are given in square brackets): main chamber $(2-5)\times 10^{-4}$ Pa [$<1\times 10^{-5}$]; stage I $(1-3)\times 10^{-6}$ Pa [6×10^{-8}]; stage II $(1-2)\times 10^{-7}$ Pa [4×10^{-8}]. The pressure increment in the exit mirror box of the TGM was noted to be $(1-4)\times 10^{-9}$ Pa, and the increment in the grating chamber was estimated to be 10^{-11} Pa.

An automatic valve ($V3$) can be introduced between the last pumping stage and the monochromator to provide rapid isolation of the electron spectrometer and photon source in case of a vacuum failure in either part. A special valve ($V2$) allows the separation of the main chamber and differential pumping stages and, if needed, the introduction of a thin foil.

The use of two analyzers increases the data acquisition rate twofold, or allows the convenient recording of reference data simultaneously with a measurement. As a special feature, the asymmetry parameter β can be determined without rotating the analyzers, once the symmetry of the system as well as the validity of the dipole approximation for the case under study have been established.

Using a photon beam with the polarization p, the angular distribution of photoelectrons is given in the dipole approximation by

$$\frac{d\sigma}{d\Omega}=\frac{\sigma}{4\pi}\left(1+\frac{\beta}{4}(1+3p\cos 2\theta)\right), \tag{1}$$

where θ is the angle relative to the major electric vector of the polarized photon beam, β the asymmetry parameter, and σ the photoionization cross section. The differential cross section $d\sigma/d\Omega$ is proportional to the observed photoelectron intensity, $I(\theta)$, and by measuring $I(\theta)$ at $\theta=0°$ and $\theta=90°$, the β parameter is obtained from

$$\beta=\frac{4(R-1)}{3p(R+1)-(R-1)} \tag{2}$$

where $R=I(0°)/I(90°)$.

In the present experiment, only one of the analyzers was used and rotated into the 0° and 90° positions. The symmetry about the photon axis of all parameters affecting the origin and path of the photoelectrons was checked and verified by recording angular distributions of He 1s and Xe 5p electrons in small angular increments between −90° and +180°. At pressures of less than 6×10^{-4} Pa in the main chamber, corresponding to about 6×10^{-2} Pa in the source cell, intensity ratios and β parameters were found to be independent of pressure. Data were recorded generally at (2 to 4)$\times 10^{-4}$ Pa in the main chamber.

The polarization of the photon beam was obtained from a measurement of the He 1s angular distribution [Eq. (2)] assuming $\beta = 2$ at all energies. For the 450-l/mm low-energy grating (LEG), we found $p = 0.93(1)$ for $25 < h\nu < 50$ eV, and for the 1800-l/mm high-energy grating (HEG), p decreased monotonically from 0.92(1) at $h\nu = 40$ eV to 0.84(1) at $h\nu = 105$ eV. These values are slightly lower than those measured previously for a similar TGM.[9]

Data could be recorded in the constant acceleration mode or the constant pass-energy mode, but were usually obtained by setting the pass energy to either 14 or 35 eV (with $\Delta E/E = 1.5\%$) and scanning the electron source with a 50-ms ramp voltage that was synchronized with the channel advance of a multiscaler. Under these conditions, the Xe 5p doublet was sufficiently well resolved and count rates were sufficiently high to ensure reliability in the various necessary corrections and acceptable statistical confidence in relatively short acquisition times. The photon bandpass was about 5 Å for the LEG and 1 Å for the HEG. As an example, 3×10^5 counts were accumulated in the Xe $5p_{3/2}$ peak and a signal-to-background ratio of 70:1 was obtained under the following conditions: $\theta = 0°$, $h\nu = 21.2$ eV, 100 mA beam current, 7 Å bandpass, 14 eV pass energy, 0.28 eV FWHM of photoline, about 3×10^{-2} Pa of Xe in the source, 256 data channel, and an acquisition time of 100s over a 4-eV energy scan.

RESULTS AND DISCUSSION

Photoelectron spectra of the Xe 5p doublet are shown in Fig. 2 for photon energies of 24.4 and 80.3 eV at the two angles, $\theta = 0°$ and 90°, chosen to obtain β from Eq. (2). The doublet is seen to be well resolved. The β parameters of the two spin-orbit components are given in Table I and plotted in Fig. 3 together with the values of Dehmer *et al.*[3] below 40 eV and the data of Torop *et al.*[4] above 60 eV. The latter data represent an average of the doublet component values. Our data are the average of two to three runs per point. The errors take into account the statistical uncertainties, and the uncertainties in the polarization measurement and the analysis procedure. At $h\nu = 55.3$ eV, the parameter β could be determined only for the $5p_{1/2}$ component, because the $5p_{3/2}$ line was buried under the $4d_{5/2}$ line excited by second-order radiation. Between 35 and 45 eV Auger lines excited by second-order photons could be present, but their effect was minimized by using the 450-l/mm LEG and by appropriate selection of the photon energies. As a consequence, the weak Auger lines which did appear overlapped only slightly with the ^2P lines, and their contributions could be removed.

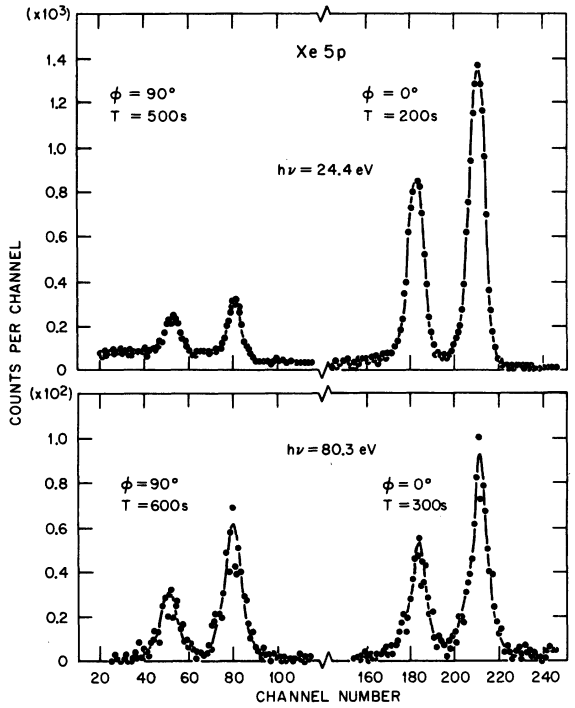

FIG. 2. Typical photoelectron spectra of Xe 5p doublet recorded at $\theta = 0°$, and $\theta = 90°$ with the 450-lines/mm grating at 24 eV and the 1800-lines mm grating at 80 eV. Time indicated is the total recording time per spectrum.

In Fig. 4, the differences between the β component values are plotted with the few values available from other work.[3,10] The error in the

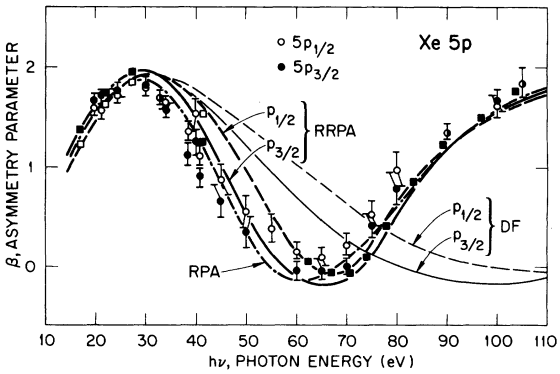

FIG. 3. The asymmetry parameter β for the Xe 5p doublet. Our data: • for $^2P_{3/2}$ and o for $^2P_{1/2}$; Dehmer, *et al.* (Ref. 3): □,■ pairs for the components; and Torop *et al.* (Ref. 4): ■ for the doublet average (above 60 eV). RRPA theory is from Johnson and colleagues (Refs. 1, 8, and 11), RPA from Amusia and Ivanov (Ref. 7), and DF from Ong and Manson (Ref. 6).

TABLE I. Asymmetry parameter β for the Xe $5p$ spin-orbit components and the Xe $5p$ branching ratio.

$h\nu$ (eV)	$\beta(^2P_{1/2})$	$\beta(^2P_{3/2})$	$\frac{\sigma(^2P_{3/2})}{\sigma(^2P_{1/2})}$
19.5	1.60(6)	1.66(6)	1.60(5)
21.2	1.57(7)	1.72(7)	1.47(11)
24.4	1.73(6)	1.77(6)	1.55(4)
30.2	1.80(8)	1.81(7)	1.41(4)
32.7	1.70(7)	1.70(6)	1.45(6)
34.0	1.64(8)	1.56(8)	1.44(5)
38.4	1.36(10)	1.12(11)	1.54(5)
40.0	1.54(13)	1.25(12)	1.54(6)
41.0	1.11(10)	0.90(10)	1.51(5)
45.2	0.88(9)	0.67(11)	1.51(9)
50.2	0.57(10)	0.36(10)	1.72(12)
55.3	0.43(13)		
60.3	0.17(9)	−0.04(9)	1.91(15)
65.3	0.10(10)	−0.03(9)	1.75(10)
70.3	0.23(11)	0.02(8)	2.07(16)
75.4	0.53(12)	0.43(12)	1.81(9)
80.4	0.98(15)	0.80(15)	1.97(11)
90.4	1.35(8)	1.35(8)	1.75(9)
100.4	1.62(10)	1.66(10)	1.70(11)
105.5	1.87(15)	1.86(15)	1.52(15)

difference is about one-half the errors in the β values because several error sources affect the components similarly.

In Figs. 3 and 4, the experimental data are compared with theoretical predictions from several models: the DF model[6] which is relativistic but ignores correlations, the RPA model[7] which is nonrelativistic but considers intrashell and intershell interactions involving the $5p$, $5s$, and $4d$ shells, and the RRPA model[1,8,11] which takes both the relativistic effects and the $(5p+5s+4d)$ correlations into account. Other calculations such as the single-particle Herman-Skillman (HS)[12] and Hartree-Fock (HF)[13] predictions and the many-body RPA[14] and RRPA[1,8] predictions that consider only the $(5p+5s)$ interchannel interactions are not shown in the figures.

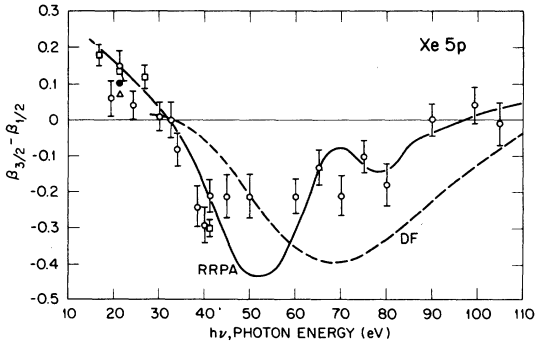

FIG. 4. The difference $\Delta\beta$ of the Xe $5p$ spin-orbit components compared with theory: RRPA (Ref. 11), DF (Ref. 6). Present data: ○; Earlier data given in Ref. 3 (□) and in Ref. 10 (●, △) are also shown.

The comparison made in Fig. 3 for β shows that there is good agreement between the experimental data and the many-body calculations that include the $(5p+5s+4d)$ correlations. The agreement between experimental and DF predictions is not good. Similarly, the HS and HF results agree poorly with the experiment, as do the RPA and RRPA results that include only the $(5p+5s)$ correlations.[1,2,8,14] The comparison then shows that the interactions between the $5p$, $5s$, and $4d$ shells are crucially important in predicting the behavior of the β parameter. The difference between the nonrelativistic and the relativistic random-phase approximations may in part reflect different numerical procedures and ionization potentials (of course, the RPA does not distinguish the spin-orbit components). However, the shift toward higher energies of the minima in β for the $^2P_{3/2}$ electrons and, especially, the $^2P_{1/2}$ electrons is a relativistic effect, according to a recent theoretical analysis.[15] In that analysis, the zeros in the dipole matrix elements for higher-Z elements were found to occur at substantially higher energies in the relativistic single-particle model than in the nonrelativistic calculation. Since the matrix elements determine the cross sections and enter into the calculations of the asymmetry parameters, quite similar shifts will be noted for both the Cooper minima and the corresponding minima in β. However, the relativistic shift is apparently counteracted by many-body interactions, if they do occur, as suggested by the fact that the experimentally observed minima, 64 and 66 eV for the $^2P_{3/2}$ and $^2P_{1/2}$ components, occur much below the energies predicted by DF calculations at about 100 and 120 eV. Barring other differences between the RPA and RRPA calculations, the relativistic effect alone would shift the minimum from 60.5 eV for the $5p$ doublet to 66 and 68 eV for the components.

The comparison made in Fig. 4 for $\Delta\beta$ between the experimental data and the two relativistic predictions, DF and RRPA, shows not unexpectedly that the difference between the asymmetry parameters of the spin-orbit components is reasonably well accounted for by the relativistic effect. This implies that by and large the correlations affect the two β components in a similar fashion. However, the inclusion of interchannel interactions leads to fine structure,[11] such as the dip at 80 eV due to $4d$ correlations, and to a contraction along the energy scale. The first crossover of the β

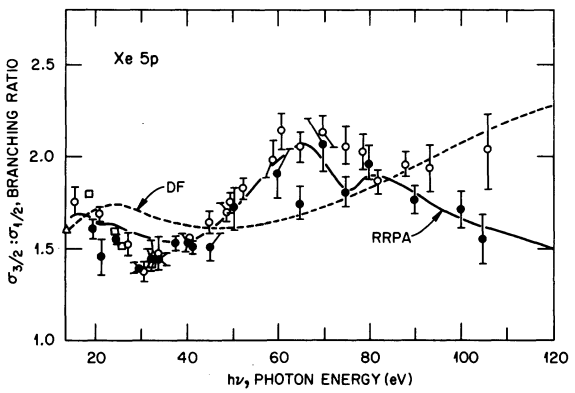

FIG. 5. The Xe $5p$ branching ratio compared with theory: RRPA (Ref. 11) and DF (Ref. 6), and previous data reported in Ref. 5. Our data are identified by solid circles (●).

values ($\Delta\beta = 0$) occurs at 31 eV in experiment and both theoretical models and the second crossover occurs between 90 and 100 eV in the experiment, at 97 eV in the RRPA and near 120 eV in the DF model. The dip in $\Delta\beta$ predicted by the RRPA at 52 eV is not fully realized by the present experiment.

To afford an additional comparison with theory, branching ratios $\sigma(^2P_{3/2})/\sigma(^2P_{1/2})$ were derived from the spectra measured at $\theta = 0°$ and the measured β parameters. The data are presented in Fig. 5 and Table I. These ratios are in good agreement with earlier data[5] up to about 80 eV, but are substantially lower toward higher energies. The DF model reproduces the gross features only; the discrepancy with experiment is much greater for the branching ratio than for the difference $\Delta\beta$, although in both cases relativity is emphasized by differentiating the spin-orbit components. The RRPA prediction is seen to be in generally good agreement with all experimental data up to about 70 eV and our data above 70 eV. A discrepancy between our datum and theory occurs at 65 eV, where the strong $4d_{5/2} \rightarrow 6p$ transition has been observed.[16] The interactions between such a discrete channel and the continuum channels are, however, not explicitly included in the RRPA calculation for Xe.

CONCLUSIONS

Study of the asymmetry parameter β of the $5p$ spin-orbit components and the determination of the branching ratio have shown that in xenon both relativistic and correlation effects are important. The dependence of β on the photon energy is influenced predominantly by the many-electron interactions, while the difference between the β parameters of the spin-orbit components reflects largely the relativistic effects. The agreement with the results of the relativistic random-phase approximation that considers intrashell and intershell correlations between the $5p$, $5s$, and $4d$ shells is good for the β parameters and the branching ratio. This type of agreement is similar to the one found previously for the Xe $5s$ asymmetry parameter, the Xe $4d$ branching ratio, partial photoionization cross sections of the Xe subshells and the similar properties in Kr.[1,2,8] Small discrepancies which appear in several places will require further experimental and theoretical scrutiny.

ACKNOWLEDGMENTS

We are indebted to W. R. Johnson for communicating to us results prior to publication. We thank the staff of the Synchrotron Radiation Center for their efficient operation of the photon source, and D. Mehaffy, P. R. Keller, J. W. Taylor, and F. A. Grimm for their help in various facets of the work. This work was sponsored by the Chemical Sciences Division, Office of Basic Energy Sciences, U. S. Department of Energy under Contract No. W-7405-eng-26 with the Union Carbide Corporation, and by the National Science Foundation under Contract No. DMR 782-1080.

[1] W. R. Johnson and K. T. Cheng, Phys. Rev. A 20, 978 (1979).
[2] M. O. Krause, in *Synchrotron Radiation Research*, edited by H. Winick and S. Doniach (Plenum, New York, 1980), Chap. 5, pp. 101–157.
[3] J. L. Dehmer, W. A. Chupka, J. Berkowitz, and W. T. Jinery, Phys. Rev. A 12, 1966 (1975).
[4] L. Torop, J. Morton, and J. B. West, J. Phys. B 9, 2034 (1976).
[5] F. Wuilleumier, M. Y. Adam, P. Dhez, N. Sandner, V. Schmidt, and W. Mehlhorn, Phys. Rev. A 16, 646 (1977).
[6] W. Ong and S. T. Manson, Phys. Rev. A 21, 842 (1980).
[7] M. Ya Amusia and V. K. Ivanov, Bull. Acad. Sci. USSR, Phys. Ser. 41, 39 (1977) [Izv. Akad. Nauk SSSR, Ser. Fiz. 41, 2509 (1977)].
[8] W. R. Johnson and C. D. Lin, Phys. Rev. A 20, 964 (1979).
[9] B. P. Tonner, Nucl. Instrum. Methods 172, 133 (1980).
[10] J. Kreile and A. Schweig, J. Electron Spectrosc. Relat. Phenom. 20, 191 (1980).
[11] K. N. Huang and W. R. Johnson (unpublished).

[12]S. T. Manson and J. W. Cooper, Phys. Rev. 165, 126 (1968).
[13]D. J. Kennedy and S. T. Manson, Phys. Rev. A 5, 227 (1972).
[14]M. Ya Amusia, in *Proceedings of the IV International Conference on VUV Rad. Physics* (Pergamon, New York, 1974), p. 205.
[15]Y. S. Kim, A. Ron, R. H. Pratt, B. R. Tambe, and S. T. Manson, Phys. Rev. Lett. 46, 1326 (1981).
[16]D. L. Ederer and M. Manalis, J. Opt. Soc. Am. 65, 634 (1975).